Cent. Eur. J. Phys. • 1-24
Author version

Central European Journal of Physics

Numerical investigation of three types of space and time fractional Bloch-Torrey equations in 2D

Research Article

Q. Yu[1], F. Liu[1,*], I. Turner[1], K. Burrage[1,2]

1 School of Mathematical Sciences, Queensland University of Technology, GPO Box 2434, Brisbane, Qld. 4001, Australia

2 Department of Computer Science and OCISB, University of Oxford, OXI 3QD,UK

Abstract: Recently, the fractional Bloch-Torrey model has been used to study anomalous diffusion in the human brain. In this paper, we consider three types of space and time fractional Bloch-Torrey equations in two dimensions: Model-1 with the Riesz fractional derivative; Model-2 with the one-dimensional fractional Laplacian operator; and Model-3 with the two-dimensional fractional Laplacian operator.
Firstly, we propose a spatially second-order accurate implicit numerical method for Model-1 whereby we discretize the Riesz fractional derivative using a fractional centered difference. We consider a finite domain where the time and space derivatives are replaced by the Caputo and the sequential Riesz fractional derivatives, respectively. Secondly, we utilize the matrix transfer technique for solving Model-2 and Model-3. Finally, some numerical results are given to show the behaviours of these three models especially on varying domain sizes with zero Dirichlet boundary conditions.

PACS (2008): 02.30.Jr, 02.60.Cb, 02.70.Bf

Keywords: fractional Bloch-Torrey equation • fractional centered difference • implicit numerical method • matrix transfer technique • bounded domains

1. Introduction

The concept of fractional calculus was first proposed by Leibniz in 1695. Since then, many famous mathematicians, such as Euler, Laplace, Fourier, Abel, Liouville, Riemann, Grünwald, Letnikov, Lévy and Riesz, have worked in this field of mathematics and provided important contributions. The main characteristic of fractional order differential equations is that they contain non-integer order derivatives [1, 2]. Fractional models can be used to describe the memory and transmissibility of many kinds of materials, and they play an increasingly important role in science and engineering [3–10]. Metzler and Klafter [4] demonstrated that fractional equations have come of age as a complementary tool in the description of anomalous transport processes. Zaslavsky [5] reviewed a new concept of fractional kinetics for systems with Hamiltonian chaos. New characteristics of the kinetics are

* *E-mail: f.liu@qut.edu.au*

extended to fractional kinetics and the most important are anomalous transport, superdiffusion and weak mixing, amongst others. Gorenflo et al. [6] derived the fundamental solution for the time fractional diffusion equation, and interpreted it as a probability density of a self-similar non-Markovian stochastic process related to the phenomenon of slow anomalous diffusion. Meerschaert and Tadjeran [7] developed practical numerical methods for solving the one-dimensional space fractional advection-dispersion equation with variable coefficients on a finite domain. The application of their results was illustrated by modelling a radial flow problem. Yu et al. [8] proposed an Adomian decomposition method to construct numerical solutions of the linear and non-linear space-time fractional reaction-diffusion equations in the form of a rapidly convergent series with easily computable components. Podlubny et al. [9] presented a matrix approach for the solution of time fractional and space fractional partial differential equations. The method is based on the idea of a net of discretisation nodes, where solutions at every desired point in time and space are found simultaneously by the solution of an appropriate linear system.

In physics and chemistry, specifically in nuclear magnetic resonance (NMR) and magnetic resonance imaging (MRI), the Bloch equations represent a set of macroscopic equations that are used for modeling the nuclear magnetization as a function of time [11]. The Bloch-Torrey equations were proposed by Torrey [12] as a generalization of the Bloch equations to describe situations when the diffusion of the spin magnetic moment is not negligible. Bhalekar et al. [13] considered transient chaos in a non-linear version of the Bloch equation that involved a radiation damping model. The fractional Bloch equation provides an opportunity to describe numerous experimental situations including heterogeneous, porous or composite materials [14, 15]. Petráš [16] proposed numerical and simulation models of the classical and fractional order Bloch equations. Magin et al. [17] considered the fractional Bloch equation to describe anomalous NMR relaxation phenomena (T_1 and T_2) in Cartilage Matrix Components. Bhalekar et al. [18] considered the fractional Bloch equation with time delays, and analysed different stability behaviors for the T_1 and the T_2 relaxation processes.

Kenkre et al. [19] proposed a simple technique for solving the Bloch-Torrey equations in the NMR study of molecular diffusion under gradient fields. Barzykin [20] derived an exact analytical solution of the Bloch-Torrey equation for restricted diffusion in a steady field gradient and, as a result, for any step-wise pulse sequence. Jochimsen et al. [21] proposed an algorithm for simulating MRI with Bloch-Torrey equations, and showed that the algorithm is efficient and decreases simulation time while retaining accuracy.

Recently, fractional order calculus has been used to examine the connection between fractional order dynamics and diffusion by solving the Bloch-Torrey equation [22–25]. It was pointed out that a fractional diffusion model could be successfully applied to analyzing diffusion images of human brain tissues and provides new insights into further investigations of other tissue structures and the micro-environment.

Magin et al. [24] proposed a new diffusion model for solving the Bloch-Torrey equation using fractional order calculus with respect to time and space (ST-FBTE):

$$\tau^{\alpha-1}\ {}_0^C D_t^\alpha M_{xy}(\mathbf{r},t) = \lambda M_{xy}(\mathbf{r},t) + D\mu^{2(\beta-1)}\mathbf{R}^\beta M_{xy}(\mathbf{r},t), \tag{1}$$

where $\lambda = -i\gamma(\mathbf{r}\cdot\mathbf{G}(t))$, $\mathbf{r} = (x, y, z)$, $\mathbf{G}(t)$ is the magnetic field gradient, γ and D are the gyromagnetic ratio and the diffusion coefficient, respectively. ${}_0^C D_t^\alpha$ is the Caputo time fractional derivative of order α $(0 < \alpha \leq 1)$ with respect to t, and with the starting point at $t = 0$ is defined as [2]:

$$ {}_0^C D_t^\alpha M(x, y, z, t) = \frac{1}{\Gamma(1-\alpha)} \int_0^t \frac{M'(x, y, z, \tau)}{(t-\tau)^\alpha} d\tau. \tag{2} $$

$M_{xy}(\mathbf{r}, t) = M_x(\mathbf{r}, t) + iM_y(\mathbf{r}, t)$, where $i = \sqrt{-1}$, comprises the transverse components of the magnetization; and $\tau^{\alpha-1}$ and $\mu^{2(\beta-1)}$ are the fractional order time and space constants needed to preserve units, $(0 < \alpha \leq 1$, and $1 < \beta \leq 2)$. Magin et al. [24] considered $\mathbf{R}^\beta = (R_x^\beta + R_y^\beta + R_z^\beta)$ as a sequential Riesz fractional order operator in space [2], and some authors [26–29] proposed to study the fractional Laplacian operator formulation replacing the Riesz fractional derivative. In this paper, we consider three types of space and time fractional Bloch-Torrey equations in two dimensions (ST-FBTE2D), namely, Model-1: ST-FBTE2D with the Riesz fractional derivative; Model-2: ST-FBTE2D with the one-dimensional fractional Laplacian operator, and Model-3: the space fractional Bloch-Torrey equation with a two-dimensional fractional Laplacian operator.

Compared with the considerable work carried out on theoretical analysis, little work has been done on the numerical solution of equation (1). Magin et al. [24] derived analytical solutions with fractional order dynamics in space (i.e., $\alpha = 1$ and $1 < \beta \leq 2$) and time (i.e., $0 < \alpha < 1$ and $\beta = 2$). Zhou et al. [31] applied the results from [30] to analyze diffusion images of healthy human brain tissues in vivo successfully at high b values up to 4700 sec/mm^2. Yu et al. [23] derived an analytical solution and an effective implicit numerical method for solving equation (1), and also considered the stability and convergence properties of the implicit numerical method. However, due to computational overheads necessary to perform the simulations for ST-FBTE in three dimensions, Yu et al. [23] presented a preliminary study based on a two-dimensional example to confirm their theoretical analysis. Yu et al. [22] proposed a fractional alternating direction implicit scheme to overcome this problem, they also proved the stability and convergence of the proposed method with order of convergence one in space.

For the Riesz fractional formulation, the Grünwald-Letnikov derivative approximation scheme of order one can be used [22, 23, 30–32]. However, in order to better approximate the Riesz fractional derivative, Ortigueira [33] defined a 'fractional centered derivative' and proved that the Riesz fractional derivative of an analytic function can be represented by the fractional centered derivative. Celik and Duman [34] used the fractional centered derivative to approximate the Riesz fractional derivative and applied the Crank-Nicolson method to a fractional diffusion equation in the Riesz formulation, and showed that the method is unconditionally stable and convergent with accuracy two.

In this paper, we use the fractional centered derivative to approximate the Riesz fractional derivative in Model-1 which can obtain second order accuracy in space, and propose an implicit numerical method. In addition, the matrix transfer technique for solving Models 2 and 3 is investigated.

The remainder of this paper is arranged as follows. Some mathematical preliminaries are introduced in Section 2.

In Section 3, we propose an implicit numerical method for Model-1. The Matrix transform technique for Models 2 and 3 is demonstrated in Sections 4 and 5, respectively. Finally, some numerical results are given to assess the behaviours of these models on varying domain sizes with zero Dirichlet boundary conditions.

2. Preliminary knowledge

In this section, we outline some preliminary knowledge used throughout the remaining sections of this paper. It is assumed throughout this section that $M(x,y,t) \in C^{3,3,2}_{x,y,t}(\Omega)$ for $0 < \alpha \leq 1$ and $1 < \beta \leq 2$, where $t \in [0,T]$ and $\Omega : -\infty \leq x, y \leq +\infty$.

Definition 2.1.
Let M be as defined above on an infinite interval $\Omega : -\infty \leq x, y \leq +\infty$. The Riesz fractional operator $\mathbf{R}^{\beta}$ is defined as [27]

$$R^{\beta}_{x} M(x,y,t) = \frac{\partial^{\beta} M(x,y,t)}{\partial |x|^{\beta}} = -c_{\beta}({}_{-\infty}D^{\beta}_{x} + {}_{x}D^{\beta}_{+\infty}) M(x,y,t), \tag{3}$$

where $c_{\beta} = \frac{1}{2\cos(\frac{\pi\beta}{2})}$, $\beta \neq 1$,

$$\begin{aligned} {}_{-\infty}D^{\beta}_{x} M(x,y,t) &= \frac{1}{\Gamma(2-\beta)} \frac{\partial^2}{\partial x^2} \int_{-\infty}^{x} \frac{M(\xi,y,t)d_{\xi}}{(x-\xi)^{\beta-1}}, \\ {}_{x}D^{\beta}_{+\infty} M(x,y,t) &= \frac{(-1)^2}{\Gamma(2-\beta)} \frac{\partial^2}{\partial x^2} \int_{x}^{+\infty} \frac{M(\xi,y,t)d_{\xi}}{(\xi-x)^{\beta-1}}. \end{aligned}$$

Similarly, we can define the Riesz fractional derivatives $R^{\beta}_{y} M(x,y,t) = \frac{\partial^{\beta} M(x,y,t)}{\partial |y|^{\beta}}$ of order β $(1 < \beta \leq 2)$ with respect to y.

Lemma 2.1.
Suppose that $M(x) \in C^3(-\infty, \infty)$, the following equality holds

$$\frac{\partial^{\beta}}{\partial |x|^{\beta}} M(x) = -\frac{1}{2\cos\frac{\pi\beta}{2}} [{}_{-\infty}D^{\beta}_{x} + {}_{x}D^{\beta}_{+\infty}] M(x), \tag{4}$$

where $1 < \beta \leq 2$.

Proof. See [30, 31]. □

Lemma 2.2.
Suppose that $M(x) \in C^3[0,L]$, the following equality

$$\frac{\partial^{\beta}}{\partial |x|^{\beta}} M(x) = -\frac{1}{2\cos\frac{\pi\beta}{2}} [{}_{0}D^{\beta}_{x} + {}_{x}D^{\beta}_{L}] M^{*}(x), \tag{5}$$

also holds when setting

$$M^{*}(x) = \begin{cases} M(x), & x \in (0,L), \\ 0, & x \notin (0,L), \end{cases}$$

i.e., $M^{*}(x) = 0$ on the boundary points and beyond the boundary points.

Proof. See [30, 31]. □

The use of Lemmas 1 and 2 above allows us to define the Riesz fractional operator on a bounded set Ω with zero Dirichlet boundary conditions.

Definition 2.2.
[26] Suppose the one-dimensional Laplacian $(-\Delta)$ has a complete set of orthonormal eigenfunctions φ_n corresponding to eigenvalues λ_n^2 on a bounded region $\Omega = [0, L]$, i.e., $(-\Delta)\varphi_n = \lambda_n^2\varphi_n$ on a bounded region Ω; $\mathcal{B}(\varphi) = 0$ on $\partial\Omega$, where $\mathcal{B}(\varphi)$ represents homogeneous Dirichlet boundary condition. Let

$$\mathcal{F} = \left\{ f = \sum_{n=1}^{\infty} c_n\varphi_n,\ c_n = \langle f, \varphi_n\rangle, \sum_{n=1}^{\infty} |c_n|^2|\lambda_n|^{2\beta} < \infty,\ 1 < \beta \le 2 \right\},$$

then for any $f \in \mathcal{F}$, $(-\Delta)^{\frac{\beta}{2}}$ is defined by

$$(-\Delta)^{\frac{\beta}{2}} f = \sum_{n=1}^{\infty} c_n(\lambda_n^2)^{\frac{\beta}{2}}\varphi_n, \tag{6}$$

where $\lambda_n^2 = \frac{n^2\pi^2}{L^2}$ for $n = 1, 2, \cdots$, and the corresponding eigenfunctions are nonzero constant multiples of $\varphi_n = \sin\frac{n\pi x}{L}$.

Definition 2.3.
[27] Suppose the two-dimensional Laplacian $(-\Delta)$ has a complete set of orthonormal eigenfunctions $\varphi_{n,m}$ corresponding to eigenvalues $\lambda_{n,m}^2$ in a rectangular region $\Omega = [0, L_1] \times [0, L_2]$, i.e., $(-\Delta)\varphi_{n,m} = \lambda_{n,m}^2\varphi_{n,m}$ on Ω; $\mathcal{B}(\varphi) = 0$ on $\partial\Omega$, where $\mathcal{B}(\varphi)$ is the standard homogeneous Dirichlet boundary condition. Let

$$\mathcal{F} = \left\{ f = \sum_{n=1}^{\infty}\sum_{m=1}^{\infty} c_{n,m}\varphi_{n,m}, \quad c_{n,m} = \langle f, \varphi_{n,m}\rangle, \quad \sum_{n=1}^{\infty}\sum_{m=1}^{\infty} |c_{n,m}|^2|\lambda_{n,m}|^{2\beta} < \infty, \quad 1 < \beta \le 2 \right\},$$

then for any $f \in \mathcal{F}$, the two-dimensional fractional Laplacian $(-\Delta)^{\beta/2}$ is defined by

$$(-\Delta)^{\beta/2} f = \sum_{n=1}^{\infty}\sum_{m=1}^{\infty} c_{n,m}(\lambda_{n,m}^2)^{\frac{\beta}{2}}\varphi_{n,m}, \tag{7}$$

where $\lambda_{n,m}^2 = \frac{n^2\pi^2}{L_1^2} + \frac{m^2\pi^2}{L_2^2}$, and $\varphi_{n,m} = \sin\frac{n\pi x}{L_1}\sin\frac{m\pi y}{L_2}$ are the eigenvalues and corresponding eigenfunctions of the three-dimensional Laplacian $(-\Delta)$ for $n, m = 1, 2, \ldots$.

We present our solution techniques for solving the following three types of ST-FBTE2D.

Model-1: the ST-FBTE2D with Riesz formulation is rewritten in the form, with now $\mathbf{r} = (x, y)$, as

$$K_\alpha\ {}_0^C D_t^\alpha M_{xy}(\mathbf{r}, t) = \lambda M_{xy}(\mathbf{r}, t) + K_\beta \mathbf{R}_1^\beta M_{xy}(\mathbf{r}, t), \tag{8}$$

where $\mathbf{R}_1^\beta = (\frac{\partial^\beta}{\partial|x|^\beta} + \frac{\partial^\beta}{\partial|y|^\beta})$. We equate real and imaginary components to express equation (8) as a coupled system of partial differential equations for the components M_x and M_y with $\lambda_G = \gamma(\mathbf{r}\cdot\mathbf{G}(t))$, namely

$$K_\alpha\ {}_0^C D_t^\alpha M_x(\mathbf{r}, t) = \lambda_G M_y(\mathbf{r}, t) + K_\beta(\frac{\partial^\beta}{\partial|x|^\beta} + \frac{\partial^\beta}{\partial|y|^\beta})M_x(\mathbf{r}, t), \tag{9}$$

$$K_\alpha\ {}_0^C D_t^\alpha M_y(\mathbf{r}, t) = -\lambda_G M_x(\mathbf{r}, t) + K_\beta(\frac{\partial^\beta}{\partial|x|^\beta} + \frac{\partial^\beta}{\partial|y|^\beta})M_y(\mathbf{r}, t). \tag{10}$$

For convenience, ST-FBTEs (9) and (10) are decoupled (see [35]), which is equivalent to solving a fractional in space and time partial differential equation of the form

$$K_\alpha \, {}_0^C D_t^\alpha M(\mathbf{r},t) = K_\beta(\frac{\partial^\beta}{\partial|x|^\beta} + \frac{\partial^\beta}{\partial|y|^\beta})M(\mathbf{r},t) + f(\mathbf{r},t), \tag{11}$$

where M can be either M_x or M_y, and $f(\mathbf{r},t) = \lambda_G M_y(\mathbf{r},t)$ if $M = M_x$, and $f(\mathbf{r},t) = -\lambda_G M_x(\mathbf{r},t)$ if $M = M_y$.
Model-2: the ST-FBTE2D with the one-dimensional fractional Laplacian operator could be written as

$$K_\alpha \, {}_0^C D_t^\alpha M_{xy}(\mathbf{r},t) = \lambda M_{xy}(\mathbf{r},t) + K_\beta \mathbf{R}_2^\beta M_{xy}(\mathbf{r},t), \tag{12}$$

with $\mathbf{R}_2^\beta = -\left[(-\Delta_x)^{\frac{\beta}{2}} + (-\Delta_y)^{\frac{\beta}{2}}\right]$, where $\Delta_x = \frac{\partial^2}{\partial x^2}$ and $\Delta_y = \frac{\partial^2}{\partial y^2}$.
Similarly, equation (12) could be written as:

$$K_\alpha \, {}_0^C D_t^\alpha M(\mathbf{r},t) = -K_\beta \left[(-\Delta_x)^{\frac{\beta}{2}} + (-\Delta_y)^{\frac{\beta}{2}}\right] M(\mathbf{r},t) + f(\mathbf{r},t). \tag{13}$$

Model-3: the space fractional Bloch-Torrey equation in two dimensions with the two-dimensional fractional Laplacian operator, could be written as

$$\frac{\partial M(\mathbf{r},t)}{\partial t} = -K_\beta(-\Delta)^{\frac{\beta}{2}} M(\mathbf{r},t) + f(\mathbf{r},t), \tag{14}$$

where $\Delta = \frac{\partial^2}{\partial x^2} + \frac{\partial^2}{\partial y^2}$.

3. An implicit numerical method for Model-1

We propose an implicit numerical method for solving Model-1 with initial and zero Dirichlet boundary conditions on a finite domain given by

$$K_\alpha \, {}_0^C D_t^\alpha M(\mathbf{r},t) = K_\beta(\frac{\partial^\beta}{\partial|x|^\beta} + \frac{\partial^\beta}{\partial|y|^\beta})M(\mathbf{r},t) + f(\mathbf{r},t), \tag{15}$$

$$M(\mathbf{r},0) = M_0(\mathbf{r}), \tag{16}$$

$$M(\mathbf{r},t)|_{\bar{\Omega}} = 0, \tag{17}$$

where $0 < \alpha \leq 1$, $1 < \beta \leq 2$, $0 < t \leq T$, $\mathbf{r} = (x,y) \in \Omega$, Ω is the finite rectangular region $[0, L_1] \times [0, L_2]$, $M_0(\mathbf{r}) = M_0(x,y)$ is continuous on Ω, $\bar{\Omega}$ is $\mathcal{R}^2 - \Omega$.
Suppose that the continuous problem (15)-(17) has a smooth solution $M(x,y,t) \in C_{x,y,t}^{3,3,2}(\Omega)$. Let $h_x = L_1/N_1, h_y = L_2/N_2$, and $\tau = T/N$ be the spatial and time steps, respectively. At a point (x_i, y_j) at the moment of time t_n for $i,j \in \mathcal{N}$ and $n \in \mathcal{N}$, we denote the exact and numerical solutions of $M(\mathbf{r},t)$ as $u(x_i, y_j, t_n)$ and $u_{i,j}^n$, respectively.

Firstly, we discretize the Caputo time fractional derivative of $u(x_i, y_j, t_{n+1})$ by adopting the scheme in [32] as

$$ {}_0^C D_t^\alpha u(x_i, y_j, t)|_{t=t_{n+1}} = \frac{\tau^{-\alpha}}{\Gamma(2-\alpha)} \sum_{l=0}^{n} b_l [u(x_i, y_j, t_{n+1-l}) - u_(x_i, y_j, t_{n-l})] + O(\tau^{2-\alpha}), \tag{18} $$

where $b_l = (l+1)^{1-\alpha} - l^{1-\alpha}$, $l = 0, 1, \cdots, N$.

Secondly, we discretize the Riesz fractional derivative using the fractional centered difference scheme given in [34]

$$ \frac{\partial^\beta}{\partial |x|^\beta} u(x, y_j, t_{n+1})|_{x=x_i} = -\frac{1}{h_x^\beta} \sum_{p=-N_1+i}^{i} \omega_p u(x_{i-p}, y_j, t_{n+1}) + O(h_x^2), \tag{19} $$

where the coefficients ω_p are defined by

$$ \omega_p = \frac{(-1)^p \Gamma(\beta+1)}{\Gamma(\frac{\beta}{2} - p + 1)\Gamma(\frac{\beta}{2} + p + 1)}, p = 0, \mp 1, \mp 2, \cdots. \tag{20} $$

Similarly,

$$ \frac{\partial^\beta}{\partial |y|^\beta} u(x_i, y, t_{n+1})|_{y=y_j} = -\frac{1}{h_y^\beta} \sum_{q=-N_2+j}^{j} \omega_q u(x_i, y_{j-q}, t_{n+1}) + O(h_y^2). \tag{21} $$

Thus, we can derive the implicit numerical scheme:

$$ \frac{K_\alpha \tau^{-\alpha}}{\Gamma(2-\alpha)} \sum_{l=0}^{n} b_l (u_{i,j}^{n+1-l} - u_{i,j}^{n-l}) = -K_\beta \left(\frac{1}{h_x^\beta} \sum_{p=-N_1+i}^{i} \omega_p u_{i-p,j}^{n+1} + \frac{1}{h_y^\beta} \sum_{q=-N_2+j}^{j} \omega_q u_{i,j-q}^{n+1} \right) + f_{i,j}^n. \tag{22} $$

We then can obtain the following implicit difference approximation:

$$ \begin{aligned} & u_{i,j}^{n+1} + \mu_1 \sum_{p=-N_1+i}^{i} \omega_p u_{i-p,j}^{n+1} + \mu_2 \sum_{q=-N_2+j}^{j} \omega_q u_{i,j-q}^{n+1} = \sum_{l=0}^{n-1} (b_l - b_{l+1}) u_{i,j}^{n-l} + b_n u_{i,j}^0 + \mu_0 f_{i,j}^n, \\ & i = 1, 2, \cdots, N_1 - 1, j = 1, 2, \cdots, N_2 - 1, \end{aligned} \tag{23} $$

with

$$ \begin{aligned} & u_{i,j}^0 = M_0(x_i, y_j), \quad u_{0,j}^{n+1} = u_{N_1,j}^{n+1} = u_{i,0}^{n+1} = u_{i,N_2}^{n+1} = 0, \\ & (i = 0, 1, \cdots, N_1, j = 0, 1, \cdots, N_2), \end{aligned} $$

where $\mu_0 = \frac{\tau^\alpha \Gamma(2-\alpha)}{K_\alpha}$, $\mu_1 = \frac{K_\beta \tau^\alpha \Gamma(2-\alpha)}{K_\alpha h_x^\beta}$, $\mu_2 = \frac{K_\beta \tau^\alpha \Gamma(2-\alpha)}{K_\alpha h_y^\beta}$, and noting that coefficients μ_0, μ_1, $\mu_2 > 0$ for $0 < \alpha \leq 1$ and $1 < \beta \leq 2$.

Lemma 3.1.
The coefficients b_l, $l = 0, 1, 2, \cdots$ satisfy:

1. *$b_0 = 1$, $b_l > 0$ for $l = 1, 2, \cdots$;*
2. *$b_l > b_{l+1}$ for $l = 0, 1, 2, \cdots$.*

Proof. See [36]. □

Lemma 3.2.
The coefficients ω_p $(p \in \mathcal{N})$ satisfy:

1. $\omega_0 \geq 0$, $\omega_{-k} = \omega_k \leq 0$ *for all* $|k| \geq 1$;
2. $\sum_{p=-\infty}^{\infty} \omega_p = 0$;
3. *For any positive integer* n, m *with* $n < m$, *we have* $\sum_{p=-m+n}^{n} \omega_p > 0$.

Proof. See [33, 34]. □

3.1. Stability of the implicit numerical method

Let $\widetilde{u}_{i,j}^n$ be the approximate solution of the implicit numerical method (23). Setting $\varepsilon_{i,j}^n = u_{i,j}^n - \widetilde{u}_{i,j}^n$, and $\mathbf{E}^n = [\varepsilon_{1,1}^n, \varepsilon_{2,1}^n, \cdots, \varepsilon_{N_1-1,N_2-1}^n]^T$.

Assuming $\|\mathbf{E}^n\|_\infty = \max_{1\leq i\leq N_1-1, 1\leq j\leq N_2-1} |\varepsilon_{i,j}^n|$, and using mathematical induction, we have the following theorem.

Theorem 3.1.
The implicit difference approximation defined by (23) is unconditionally stable, and

$$\|\mathbf{E}^{n+1}\|_\infty \leq \|\mathbf{E}^0\|_\infty, \qquad n = 0, 1, 2, \cdots, N.$$

Proof. According to (23), the error $\varepsilon_{i,j}^n$ satisfies

$$\varepsilon_{i,j}^{n+1} + \mu_1 \sum_{p=-N_1+i}^{i} \omega_p \varepsilon_{i-p,j}^{n+1} + \mu_2 \sum_{q=-N_2+j}^{j} \omega_q \varepsilon_{i,j-q}^{n+1} = \sum_{l=0}^{n-1} (b_l - b_{l+1}) \varepsilon_{i,j}^{n-m} + b_n \varepsilon_{i,j}^0, \tag{24}$$

for $i = 1, 2, \cdots, N_1 - 1, j = 1, 2, \cdots, N_2 - 1$.

When $n = 0$, assume that $\|\mathbf{E}^1\|_\infty = \max_{1\leq i\leq N_1-1, 1\leq j\leq N_2-1} |\varepsilon_{i,j}^1| = |\varepsilon_{i_*,j_*}^1|$. With the well known inequality $|Z_1| -$

$|Z_2| \le |Z_1 - Z_2|$, using Lemmas 3.1 and 3.2, and noting that $\mu_1, \mu_2 > 0$ we have

$$
\begin{aligned}
& \|\mathbf{E}^1\|_\infty = |\varepsilon^1_{i_*,j_*}| \\
\le\ & |\varepsilon^1_{i_*,j_*}| + \mu_1 \sum_{p=-N_1+i_*}^{i_*} \omega_p |\varepsilon^1_{i_*,j_*}| + \mu_2 \sum_{q=-N_2+j_*}^{j_*} \omega_q |\varepsilon^1_{i_*,j_*}| \\
=\ & [1+\omega_0(\mu_1+\mu_2)]|\varepsilon^1_{i_*,j_*}| + \mu_1 \sum_{p=-N_1+i_*,p\neq 0}^{i_*} \omega_p |\varepsilon^1_{i_*,j_*}| + \mu_2 \sum_{q=-N_2+j_*,q\neq 0}^{j_*} \omega_q |\varepsilon^1_{i_*,j_*}| \\
\le\ & [1+\omega_0(\mu_1+\mu_2)]|\varepsilon^1_{i_*,j_*}| + \mu_1 \sum_{p=-N_1+i_*,p\neq 0}^{i_*} \omega_p |\varepsilon^1_{i_*-p,j_*}| + \mu_2 \sum_{q=-N_2+j_*,q\neq 0}^{j_*} \omega_q |\varepsilon^1_{i_*,j_*-q}| \\
\le\ & \left| [1+\omega_0(\mu_1+\mu_2)]\varepsilon^1_{i_*,j_*} + \mu_1 \sum_{p=-N_1+i_*,p\neq 0}^{i_*} \omega_p \varepsilon^1_{i_*-p,j_*} + \mu_2 \sum_{q=-N_2+j_*,q\neq 0}^{j_*} \omega_q \varepsilon^1_{i_*,j_*-q} \right| \\
=\ & \left| \varepsilon^1_{i_*,j_*} + \mu_1 \sum_{p=-N_1+i_*}^{i_*} \omega_p \varepsilon^1_{i_*-p,j_*} + \mu_2 \sum_{q=-N_2+j_*}^{j_*} \omega_q \varepsilon^1_{i_*,j_*-q} \right| \\
=\ & |b_0 \varepsilon^0_{i_*,j_*}| \\
\le\ & \|\mathbf{E}^0\|_\infty.
\end{aligned}
$$

Now, suppose that $\|\mathbf{E}^m\|_\infty \le \|\mathbf{E}^0\|_\infty, m = 1, 2, \cdots, n$. By assuming that $\|\mathbf{E}^{n+1}\|_\infty = \max\limits_{1\le i\le N_1-1, 1\le j\le N_2-1} |\varepsilon^{n+1}_{i,j}| = |\varepsilon^{n+1}_{i_*,j_*}|$, using Lemmas 3.1 and 3.2 we have

$$
\begin{aligned}
& \|\mathbf{E}^{n+1}\|_\infty = |\varepsilon^{n+1}_{i_*,j_*}| \\
\le\ & |\varepsilon^{n+1}_{i_*,j_*}| + \mu_1 \sum_{p=-N_1+i_*}^{i_*} \omega_p |\varepsilon^{n+1}_{i_*,j_*}| + \mu_2 \sum_{q=-N_2+j_*}^{j_*} \omega_q |\varepsilon^{n+1}_{i_*,j_*}| \\
=\ & [1+\omega_0(\mu_1+\mu_2)]|\varepsilon^{n+1}_{i_*,j_*}| + \mu_1 \sum_{p=-N_1+i_*,p\neq 0}^{i_*} \omega_p |\varepsilon^{n+1}_{i_*,j_*}| + \mu_2 \sum_{q=-N_2+j_*,q\neq 0}^{j_*} \omega_q |\varepsilon^{n+1}_{i_*,j_*}| \\
\le\ & [1+\omega_0(\mu_1+\mu_2)]|\varepsilon^{n+1}_{i_*,j_*}| + \mu_1 \sum_{p=-N_1+i_*,p\neq 0}^{i_*} \omega_p |\varepsilon^{n+1}_{i_*-p,j_*}| + \mu_2 \sum_{q=-N_2+j_*,q\neq 0}^{j_*} \omega_q |\varepsilon^{n+1}_{i_*,j_*-q}| \\
\le\ & \left| [1+\omega_0(\mu_1+\mu_2)]\varepsilon^{n+1}_{i_*,j_*} + \mu_1 \sum_{p=-N_1+i_*,p\neq 0}^{i_*} \omega_p \varepsilon^{n+1}_{i_*-p,j_*} + \mu_2 \sum_{q=-N_2+j_*,q\neq 0}^{j_*} \omega_q \varepsilon^{n+1}_{i_*,j_*-q} \right| \\
=\ & \left| \varepsilon^{n+1}_{i_*,j_*} + \mu_1 \sum_{p=-N_1+i_*}^{i_*} \omega_p \varepsilon^{n+1}_{i_*-p,j_*} + \mu_2 \sum_{q=-N_2+j_*}^{j_*} \omega_q \varepsilon^{n+1}_{i_*,j_*-q} \right| \\
=\ & \left| \sum_{l=0}^{n-1} (b_l - b_{l+1}) \varepsilon^{n-l}_{i_*,j_*} + b_n \varepsilon^0_{i_*,j_*} \right| \\
\le\ & \sum_{l=0}^{n-1} (b_l - b_{l+1}) \|\mathbf{E}^{n-l}\|_\infty + b_n \|\mathbf{E}^0\|_\infty \\
\le\ & \left(\sum_{l=0}^{n-1} (b_l - b_{l+1}) + b_n \right) \|\mathbf{E}^0\|_\infty \\
=\ & \|\mathbf{E}^0\|_\infty.
\end{aligned}
$$

Hence the implicit numerical method defined by (23) is unconditionally stable. □

3.2. Convergence of the implicit numerical method

Setting $e_{i,j}^n = u(x_i, y_j, t_n) - u_{i,j}^n$, and denoting $\mathbf{R}^n = [e_{1,1}^n, e_{2,1}^n, \cdots, e_{N_1-1,N_2-1}^n]^T$, then $\mathbf{R}^0 = \mathbf{0}$. Here $\mathbf{R}^n$ and $\mathbf{0}$ are $((N_1-1)\times(N_2-1))$ vectors, respectively.

From (15)-(23), the error $e_{i,j}^n$ satisfies to the highest order expansion terms in τ, h_x and h_y

$$e_{i,j}^{n+1} + \mu_1 \sum_{p=-N_1+i}^{i} \omega_p e_{i-p,j}^{n+1} + \mu_2 \sum_{q=-N_2+j}^{j} \omega_q e_{i,j-q}^{n+1} = \sum_{l=0}^{n-1} (b_l - b_{l+1}) e_{i,j}^{n-l} + C_1 \tau^{\alpha} (\tau^{2-\alpha} + \tau + h_x^2 + h_y^2), \tag{25}$$

for $i = 1, 2, \cdots, N_1 - 1, j = 1, 2, \cdots, N_2 - 1$.

Assuming $\|\mathbf{R}^{n+1}\|_\infty = \max\limits_{1\le i\le N_1-1, 1\le j\le N_2-1} |e_{i,j}^{n+1}|$, and using mathematical induction, we have the following theorem.

Theorem 3.2.
The implicit difference approximation defined by (23) is convergent, and there is a positive constant C^*, such that

$$\|\mathbf{R}^{n+1}\|_\infty \le C^* (\tau^{2-\alpha} + \tau + h_x^2 + h_y^2), \quad n = 0, 1, 2, \cdots, N. \tag{26}$$

Proof. When $n = 0$, assume that $\|\mathbf{R}^1\|_\infty = \max\limits_{1\le i\le N_1-1, 1\le j\le N_2-1} |e_{i,j}^1| = |e_{i_*,j_*}^1|$. Similarly, using inequality $|Z_1| - |Z_2| \le |Z_1 - Z_2|$, Lemmas 3.1 and 3.2, and noting that $\mu_1, \mu_2 > 0$, we have

$$\begin{aligned}
&\|\mathbf{R}^1\|_\infty = |e_{i_*,j_*}^1| \\
\le\ & |e_{i_*,j_*}^1| + \mu_1 \sum_{p=-N_1+i_*}^{i_*} \omega_p |e_{i_*,j_*}^1| + \mu_2 \sum_{q=-N_2+j_*}^{j_*} \omega_q |e_{i_*,j_*}^1| \\
=\ & [1 + \omega_0(\mu_1 + \mu_2)] |e_{i_*,j_*}^1| + \mu_1 \sum_{p=-N_1+i_*, p\ne 0}^{i_*} \omega_p |e_{i_*,j_*}^1| + \mu_2 \sum_{q=-N_2+j_*, q\ne 0}^{j_*} \omega_q |e_{i_*,j_*}^1| \\
\le\ & [1 + \omega_0(\mu_1 + \mu_2)] |e_{i_*,j_*}^1| + \mu_1 \sum_{p=-N_1+i_*, p\ne 0}^{i_*} \omega_p |e_{i_*-p,j_*}^1| + \mu_2 \sum_{q=-N_2+j_*, q\ne 0}^{j_*} \omega_q |e_{i_*,j_*-q}^1| \\
\le\ & \left| e_{i_*,j_*}^1 + \mu_1 \sum_{p=-N_1+i_*}^{i_*} \omega_p e_{i_*-p,j_*}^1 + \mu_2 \sum_{q=-N_2+j_*}^{j_*} \omega_q e_{i_*,j_*-q}^1 \right|.
\end{aligned}$$

Similar to the proof of the stability in Theorem 3.1, this leads to

$$\|\mathbf{R}^1\|_\infty \le C_1 \tau^{\alpha} (\tau^{2-\alpha} + \tau + h_x^2 + h_y^2) = C_1 b_0^{-1} \tau^{\alpha} (\tau^{2-\alpha} + \tau + h_x^2 + h_y^2).$$

Now, suppose that $\|\mathbf{R}^m\|_\infty \le C_1 b_{m-1}^{-1} \tau^{\alpha} (\tau^{2-\alpha} + \tau + h_x^2 + h_y^2)$, $m = 1, 2, \cdots, n$. By assuming that $\|\mathbf{R}^{n+1}\|_\infty =$

$\max\limits_{1\le i\le N_1-1,1\le j\le N_2-1}|e_{i,j}^{n+1}|=|e_{i_*,j_*}^{n+1}|$, using Lemmas 3.1, Lemma 3.2 and (25) again, we have

$$\begin{aligned}
&\|\mathbf{R}^{n+1}\|_\infty=|e_{i_*,j_*}^{n+1}|\\
\le\ &|e_{i_*,j_*}^{n+1}|+\mu_1\sum_{p=-N_1+i_*}^{i_*}\omega_p|e_{i_*,j_*}^{n+1}|+\mu_2\sum_{q=-N_2+j_*}^{j_*}\omega_q|e_{i_*,j_*}^{n+1}|\\
=\ &[1+\omega_0(\mu_1+\mu_2)]|e_{i_*,j_*}^{n+1}|+\mu_1\sum_{p=-N_1+i_*,p\neq0}^{i_*}\omega_p|e_{i_*,j_*}^{n+1}|+\mu_2\sum_{q=-N_2+j_*,q\neq0}^{j_*}\omega_q|e_{i_*,j_*}^{n+1}|\\
\le\ &[1+\omega_0(\mu_1+\mu_2)]|e_{i_*,j_*}^{n+1}|+\mu_1\sum_{p=-N_1+i_*,p\neq0}^{i_*}\omega_p|e_{i_*-p,j_*}^{n+1}|+\mu_2\sum_{q=-N_2+j_*,q\neq0}^{j_*}\omega_q|e_{i_*,j_*-q}^{n+1}|\\
\le\ &\left|e_{i_*,j_*}^{n+1}+\mu_1\sum_{p=-N_1+i_*}^{i_*}\omega_pe_{i_*-p,j_*}^{n+1}+\mu_2\sum_{q=-N_2+j_*}^{j_*}\omega_qe_{i_*,j_*-q}^{n+1}\right|\\
=\ &\left|\sum_{l=0}^{n-1}(b_l-b_{l+1})e_{i_*,j_*}^{n-l}+C_1\tau^\alpha(\tau^{2-\alpha}+\tau+h_x^2+h_y^2)\right|\\
\le\ &\sum_{l=0}^{n-1}(b_l-b_{l+1})|e_{i_*,j_*}^{n-l}|+C_1\tau^\alpha(\tau^{2-\alpha}+\tau+h_x^2+h_y^2)\\
\le\ &\left(\sum_{l=0}^{n-1}(b_l-b_{l+1})b_{n-l-1}^{-1}+1\right)C_1\tau^\alpha(\tau^{2-\alpha}+\tau+h_x^2+h_y^2)\\
\le\ &\left(\sum_{l=0}^{n-1}(b_l-b_{l+1})b_n^{-1}+1\right)C_1\tau^\alpha(\tau^{2-\alpha}+\tau+h_x^2+h_y^2)\\
=\ &\left((b_0-b_n)b_n^{-1}+1\right)C_1\tau^\alpha(\tau^{2-\alpha}+\tau+h_x^2+h_y^2)\\
=\ &C_1b_n^{-1}\tau^\alpha(\tau^{2-\alpha}+\tau+h_x^2+h_y^2).
\end{aligned}$$

We note that

$$\lim_{n\to\infty}\frac{b_n^{-1}}{n^\alpha}=\lim_{n\to\infty}\frac{n^{-\alpha}}{(n+1)^{1-\alpha}-n^{1-\alpha}}=\frac{1}{1-\alpha},$$

and there exists a positive constant C_2, such that

$$\|\mathbf{R}^{n+1}\|_\infty\le C_1C_2n^\alpha\tau^\alpha(\tau^{2-\alpha}+\tau+h_x^2+h_y^2).$$

Finally, note that $n\tau\le T$ is finite, so there exists a positive constant C^*, such that $\|\mathbf{R}^{n+1}\|_\infty\le C^*(\tau^{2-\alpha}+\tau+h_x^2+h_y^2)$ for $n=0,1,2,\cdots$.

Hence the implicit numerical method defined by (23) is convergent. □

4. The matrix transfer method for Model-2

In this section, we utilize the matrix transfer technique proposed by Ilic et al. [26] to discretize the one-dimensional fractional Laplacian operator for solving Model-2, with initial and zero Dirichlet boundary conditions on a finite

domain given by

$$K_\alpha \, {}_0^C D_t^\alpha M(\mathbf{r},t) = -K_\beta \left[(-\Delta_x)^{\frac{\beta}{2}} + (-\Delta_y)^{\frac{\beta}{2}} \right] M(\mathbf{r},t) + f(\mathbf{r},t), \tag{27}$$

$$M(\mathbf{r},0) = M_0(\mathbf{r}), \tag{28}$$

$$M(\mathbf{r},t)|_{\bar{\Omega}} = 0, \tag{29}$$

where $0 < \alpha \leq 1$, $1 < \beta \leq 2$, $0 < t \leq T$, $\mathbf{r} = (x,y) \in \Omega$, Ω is the finite rectangular region $[0, L_1] \times [0, L_2]$, $M_0(\mathbf{r}) = M_0(x,y)$ is continuous on Ω, and $\bar{\Omega}$ is $\mathcal{R}^2 - \Omega$.

Noting that the symbols $(-\Delta_x)^{\frac{\beta}{2}}$ and $(-\Delta_y)^{\frac{\beta}{2}}$ have their usual meanings as a function of one-dimensional Laplacian $(-\Delta)$, which are defined in terms of their's spectral decomposition. For boundary value problems on finite domains, discrete eigenfunction expansions are used, where Definition 2.2 is adopted.

The standard finite difference stencil with equal grid spacing in both x and y directions, i.e., $h = L_1/N_1 = L_2/N_2$, will result in the tridiagonal approximate matrix representation of the Laplacian operator $(-\Delta_x)$ and $(-\Delta_y)$, respectively, namely

$$A = m(-\Delta_x) = \frac{1}{h^2} diag(A^*, A^*, \cdots, A^*), \tag{30}$$

$$B = m(-\Delta_y) = \frac{1}{h^2} tridiag(-\mathcal{I}, B^*, -\mathcal{I}), \tag{31}$$

where m is the "coordinate" isomorphism, $A^* = tridiag(-1, 2, -1)$ and $B^* = 2\mathcal{I}$. Here $A, B \in \mathcal{R}^{(N_1-1)(N_2-1)\times(N_1-1)(N_2-1)}$, $A^*, B^* \in \mathcal{R}^{(N_1-1)\times(N_1-1)}$, and $\mathcal{I} \in \mathcal{R}^{(N_1-1)\times(N_1-1)}$ is the identity matrix.

For a real nonsingular, symmetric matrix $A_{(N_1-1)(N_2-1)\times(N_1-1)(N_2-1)}$, there exists a nonsingular matrix $P^x_{(N_1-1)(N_2-1)\times(N_1-1)(N_2-1)}$, such that $A = P^x \Lambda_x {P^x}^T$, where $\Lambda_x = diag(\lambda_1^x, \lambda_2^x, \cdots, \lambda^x_{(N_1-1)(N_2-1)})$ and $\lambda_k^x (k = 1, 2, \cdots, (N_1-1)(N_2-1))$ are the eigenvalues of A. Hence we obtain the matrix representation

$$m(-\Delta_x)^{\frac{\beta}{2}} = A^{\frac{\beta}{2}} = (P^x \Lambda_x {P^x}^T)^{\frac{\beta}{2}} = P^x \Lambda_x^{\beta/2} {P^x}^T := A^{**} = (a_{ij}). \tag{32}$$

Similarly, we have

$$m(-\Delta_y)^{\frac{\beta}{2}} = B^{\frac{\beta}{2}} = (P^y \Lambda_y {P^y}^T)^{\frac{\beta}{2}} = P^y \Lambda_y^{\beta/2} {P^y}^T := B^{**} = (b_{ij}^{**}), \tag{33}$$

where $\Lambda_y = diag(\lambda_1^y, \lambda_2^y, \cdots, \lambda^y_{(N_1-1)(N_2-1)})$ and $\lambda_k^y (k = 1, 2, \cdots, (N_1-1)(N_2-1))$ are the eigenvalues of B.

We denote the exact and numerical solutions of $M(\mathbf{r},t)$ as $u(x_i, y_j, t_n)$ and $u_{i,j}^n$, respectively, and the Caputo time fractional derivative ${}_0^C D_t^\alpha$ is discretized as in equation (18), thus together with equations (32) and (33), we can obtain the following numerical approximation of Model-2 (27)-(29) as:

$$\begin{aligned} & u_{i,j}^{n+1} + \mu \sum_{p=1}^{N_2-1} \sum_{q=1}^{N_1-1} \left(a_{(i-1)(N_1-1)+j,(p-1)(N_1-1)+q} + b^{**}_{(i-1)(N_1-1)+j,(p-1)(N_1-1)+q} \right) u_{pq}^{n+1} \\ & = \sum_{l=0}^{n-1} (b_l - b_{l+1}) u_{i,j}^{n-l} + b_n u_{i,j}^0 + \mu_0 f_{i,j}^n, \end{aligned} \tag{34}$$

where $\mu_0 = \frac{\tau^\alpha \Gamma(2-\alpha)}{K_\alpha}$, $\mu = \frac{K_\beta \tau^\alpha \Gamma(2-\alpha)}{K_\alpha}$, $i = 1, 2, \cdots, N_2 - 1$, $j = 1, 2, \cdots, N_1 - 1$ and $n = 0, 1, 2, \cdots, N-1$.

5. The matrix transfer method for Model-3

In this section, we utilize the matrix transfer technique proposed by Yang et al. [27] to discretize the two-dimensional fractional Laplacian operator for solving Model-3, with initial and zero Dirichlet boundary conditions on a finite domain given by

$$\frac{\partial M(\mathbf{r},t)}{\partial t} = -K_\beta(-\Delta)^{\frac{\beta}{2}} M(\mathbf{r},t) + f(\mathbf{r},t), \tag{35}$$

$$M(\mathbf{r},0) = M_0(\mathbf{r}), \tag{36}$$

$$M(\mathbf{r},t)|_{\bar{\Omega}} = 0, \tag{37}$$

where $\Delta = \frac{\partial^2}{\partial x^2} + \frac{\partial^2}{\partial y^2}$, $0 < \alpha \leq 1$, $1 < \beta \leq 2$, $0 < t \leq T$, $\mathbf{r} = (x,y) \in \Omega$, Ω is the finite rectangular region $[0, L_1] \times [0, L_2]$, $M_0(\mathbf{r}) = M_0(x,y)$ is continuous on Ω, and $\bar{\Omega}$ is $\mathcal{R}^2 - \Omega$.

The symbol $(-\Delta)^{\frac{\beta}{2}}$ has the usual meaning as a function of two-dimensional Laplacian $(-\Delta)$, which is defined in terms of its spectral decomposition. For boundary value problems on finite domains, discrete eigenfunction expansions are used, where Definition 2.3 is adopted.

The standard five-point finite difference stencil with equal grid spacing in both x and y directions, i.e., $h = L_1/N_1 = L_2/N_2$, will result in the block tridiagonal approximate matrix representation of the Laplacian, namely

$$A^\sharp = m(-\Delta) = \frac{1}{h^2} tridiag(-\mathcal{I}, B^\sharp, -\mathcal{I}), \tag{38}$$

where $B^\sharp = tridiag(-1, 4, -1)$. Here $A^\sharp \in \mathcal{R}^{(M_1-1)(M_2-1)\times(M_1-1)(M_2-1)}$, $B^\sharp \in \mathcal{R}^{(M_1-1)\times(M_1-1)}$, and $\mathcal{I} \in \mathcal{R}^{(M_1-1)\times(M_1-1)}$ is the identity matrix.

Similarly, for a real nonsingular, symmetric matrix $A^\sharp$, there exists a nonsingular matrix $P_{(N_1-1)(N_2-1)\times(N_1-1)(N_2-1)}$, such that $A^\sharp = P\Lambda P^T$, where $\Lambda = diag(\lambda_1, \lambda_2, \cdots, \lambda_{(N_1-1)(N_2-1)})$ and $\lambda_k (k = 1, 2, \cdots, (N_1-1)(N_2-1))$ are the eigenvalues of $A^\sharp$. Hence we obtain the matrix representation

$$m(-\Delta)^{\frac{\beta}{2}} = A^{\sharp\frac{\beta}{2}} = (P\Lambda P^T)^{\frac{\beta}{2}} = P\Lambda^{\beta/2}P^T := A^{\sharp\sharp} = (a_{ij}^{\sharp\sharp}). \tag{39}$$

Let $\tau = T/N$ be the time step, and denote the numerical solutions of $M(\mathbf{r},t)$ as $u_{i,j}^n$. Thus, discretizing the time derivative using the backward differentiation formula and using equation (39), we can obtain the following numerical approximation of Model-3 (35)-(37) as:

$$u_{i,j}^{n+1} + \tau K_\beta \sum_{p=1}^{N_2-1} \sum_{q=1}^{N_1-1} a^{\sharp\sharp}_{(i-1)(N_1-1)+j,(p-1)(N_1-1)+q} u_{pq}^{n+1} = u_{i,j}^n + \tau f_{i,j}^n, \tag{40}$$

where $i = 1, 2, \cdots, N_2 - 1$, $j = 1, 2, \cdots, N_1 - 1$ and $n = 0, 1, 2, \cdots, N - 1$.

6. Numerical results

In this section, we compare the numerical solutions of the three types of space and time fractional Bloch-Torrey equations in 2D presented throughout Sections 3-5.

In Example 6.1, we confirm the convergence order of the implicit numerical method for Model-1 and show the solution behaviours of Models-1 and 2.

Example 6.1.
Models-1 and 2 on a finite domain are considered, namely

$$Model-1: \quad K_\alpha \, {}_0^C D_t^\alpha M(\mathbf{r},t) = K_\beta \left(\frac{\partial^\beta}{\partial|x|^\beta} + \frac{\partial^\beta}{\partial|y|^\beta}\right) M(\mathbf{r},t) + f(\mathbf{r},t), \tag{41}$$

$$Model-2: \quad K_\alpha \, {}_0^C D_t^\alpha M(\mathbf{r},t) = -K_\beta \left[(-\Delta_x)^{\frac{\beta}{2}} + (-\Delta_y)^{\frac{\beta}{2}}\right] M(\mathbf{r},t) + f(\mathbf{r},t), \tag{42}$$

with zero initial and zero Dirichlet boundary conditions

$$M(\mathbf{r},0) = 0, \tag{43}$$

$$M(\mathbf{r},t)|_{\bar{\Omega}} = 0, \tag{44}$$

where

$$\begin{aligned} f(\mathbf{r},t) = {} & \frac{K_\beta t^{\alpha+\beta}}{2cos(\beta\pi/2)} \left(\left(\frac{2}{\Gamma(3-\beta)}[x^{2-\beta} + (1-x)^{2-\beta}] - \frac{12}{\Gamma(4-\beta)}[x^{3-\beta} + (1-x)^{3-\beta}] + \frac{24}{\Gamma(5-\beta)}[x^{4-\beta} \right.\right. \\ & \left. + (1-x)^{4-\beta}] \right) y^2(1-y)^2 + \left(\frac{2}{\Gamma(3-\beta)}[y^{2-\beta} + (1-y)^{2-\beta}] - \frac{12}{\Gamma(4-\beta)}[y^{3-\beta} + (1-y)^{3-\beta}] \right. \\ & \left.\left. + \frac{24}{\Gamma(5-\beta)}[y^{4-\beta} + (1-y)^{4-\beta}] \right) x^2(1-x)^2 \right) + \frac{K_\alpha \Gamma(\alpha+\beta+1)}{\Gamma(\beta+1)} t^\beta x^2(1-x)^2 y^2(1-y)^2, \end{aligned}$$

and $0 < \alpha \leq 1$, $1 < \beta \leq 2$, $0 < t \leq T$, $\mathbf{r} = (x,y) \in \Omega$, Ω is the finite rectangular region $[0,1] \times [0,1]$ and $\bar{\Omega}$ is $\mathcal{R}^2 - \Omega$.
The exact solution of this problem is $M(\mathbf{r},t) = t^{\alpha+\beta} x^2(1-x)^2 y^2(1-y)^2$, which can be verified by substituting directly into (41) or (42).
The relative error norm defined by

$$\epsilon = \sqrt{\left(\sum_{i=0}^{N_1} \sum_{j=0}^{N_2} (u_{ij}^{exact} - u_{ij}^{num})^2 \right) \Big/ \left(\sum_{i=0}^{N_1} \sum_{j=0}^{N_2} (u_{ij}^{exact})^2 \right)} \tag{45}$$

will be used to calculate the error between the exact and numerical solutions.
With $K_\alpha = K_\beta = 1.0, \alpha = 0.8$, and $\beta = 1.8$, Table 1 lists the relative error between the exact and numerical solutions obtained by the implicit numerical method for equation (41), with spatial and temporal steps $\tau^{1/2} = h_x = h_y = 1/4, 1/8, 1/16, 1/32$ at time $t = 1$.
From Table 1, it can be seen that the

$$Error\ rate = \frac{error(h)^2}{error(\frac{1}{2}h)^2} \approx 4.$$

This is in good agreement with our theoretical analysis, namely the convergence order of the implicit numerical method for equation (41) is $(\tau^{2-\alpha} + \tau + h_x^2 + h_y^2)$.
In addition, the comparison of solution profiles obtained by the implicit numerical method and the matrix transfer technique, respectively, with spatial and temporal steps $h = 1/16$, $\tau = 1/102$ at time $t = 10/102$ with $K_\alpha = K_\beta = 1.0$, $t_{final} = 1.0$ for $\alpha = 0.8$ and $\beta = 1.8$ is given in Figure 1. From Figure 1, it can be seen that the numerical solutions obtained by the matrix transfer technique applied to Model-2 are in good agreement with those by the implicit numerical method for Model-1.

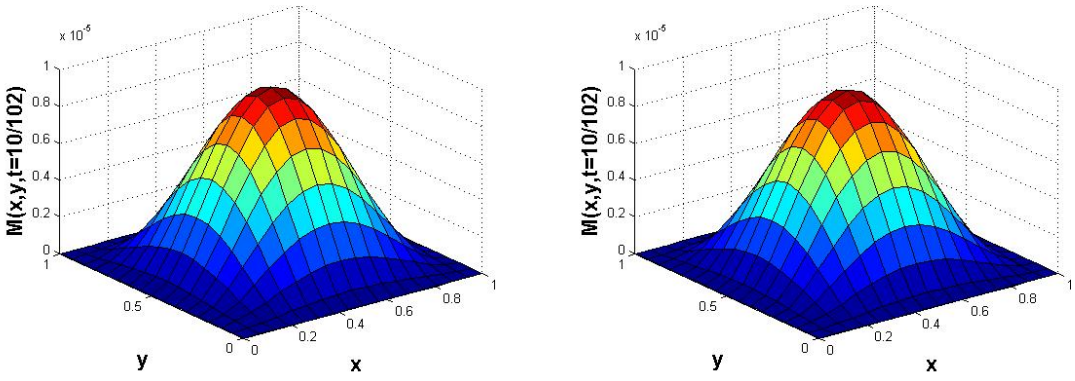

Figure 1. The comparison of solution profiles between Models-1 and 2 with spatial and temporal steps $h = 1/16$, $\tau = 1/102$ at time $t = 10/102$ with $K_\alpha = K_\beta = 1.0$, $t_{final} = 1.0$ for $\alpha = 0.8$ and $\beta = 1.8$. (a) Implicit numerical method. (b) Matrix transfer technique.

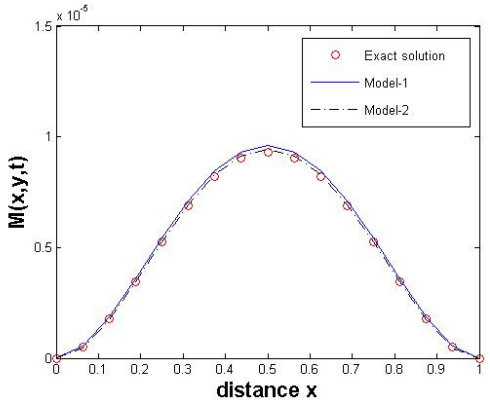

Figure 2. The comparison of solution profiles between Models-1 and 2 with spatial and temporal steps $h = 1/16$, $\tau = 1/102$ at time $t = 10/102$ with $K_\alpha = K_\beta = 1.0$, $t_{final} = 1.0$ for $y = 0.5$, $\alpha = 0.8$ and $\beta = 1.8$, and the solutions are plotted along the centre line.

Remark 6.1.
A closer comparison of solution profiles between Models-1 and 2 on the unit square with spatial and temporal steps $h = 1/16$, $\tau = 1/102$ at time $t = 10/102$ with $K_\alpha = K_\beta = 1.0$, $t_{final} = 1.0$ for $y = 0.5$, $\alpha = 0.8$ and $\beta = 1.8$ is given in Figure 2. The solutions are plotted along the centre line, and we can see that the solutions obtained from two models both close to exact solution.

Table 1. **Comparison of relative error for the implicit numerical method for Model-1 at time** $t = 1.0$

$\tau^{1/2} = h_x = h_y$	Relative error ϵ	Error rate
1/4	0.19893660	-
1/8	0.04694709	4.24
1/16	0.01113693	4.22
1/32	0.00262580	4.24

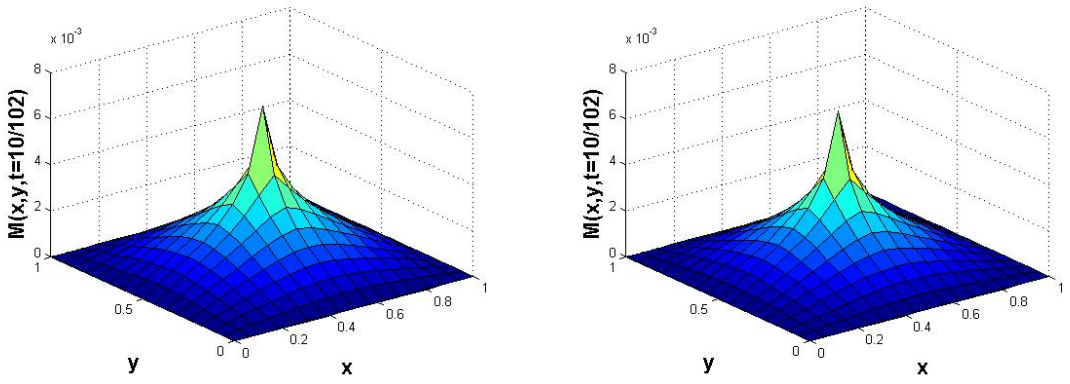

(a) (b)

Figure 3. The comparison of solution profiles between Models-1 and 2 with a nonlinear source term with spatial and temporal steps $h = 1/16$, $\tau = 1/102$ at time $t = 10/102$ with $K_\alpha = K_\beta = 1.0$, $t_{final} = 1.0$ for $\alpha = 0.8$ and $\beta = 1.8$. (a) Implicit numerical method. (b) Matrix transfer technique.

We now exhibit in Example 6.2 a comparison of the numerical solutions between Models-1 and 2 with a nonlinear source term. We also investigate the equivalence of the two models further, by studying the solution behaviour as the solution domain is extended.

Example 6.2.
We now consider problems (41) and (42) with an initial source term and zero Dirichlet boundary conditions given by

$$M(\mathbf{r}, 0) = \delta(x - 0.5, y - 0.5), \tag{46}$$
$$M(\mathbf{r}, t)|_{\bar{\Omega}} = 0, \tag{47}$$

where the nonlinear source term $f(M, \mathbf{r}, t)$ is Fisher's growth equation $f(M, \mathbf{r}, t) = 0.25M(\mathbf{r}, t)[1 - M(\mathbf{r}, t)]$, and $0 < \alpha \leq 1$, $1 < \beta \leq 2$, $0 < t \leq T$, $\mathbf{r} = (x, y) \in \Omega$, Ω is the finite rectangular region $[0, 1] \times [0, 1]$ and $\bar{\Omega}$ is $\mathcal{R}^2 - \Omega$. The comparison of solution profiles obtained by the implicit numerical method and matrix transfer technique, respectively, with spatial and temporal steps $h = 1/16$, $\tau = 1/102$ at time $t = 10/102$ with $K_\alpha = K_\beta = 1.0$, $t_{final} = 1.0$ and for $\alpha = 0.8, \beta = 1.8$ and $\alpha = 0.5, \beta = 1.5$ are given in Figures 3 and 4, respectively. We see that as α and β are reduced the profiles become more spiky, and that the numerical solutions obtained by the matrix transfer technique are in good agreement with those by the implicit numerical method.
In order to see the effect of domain size on the difference between the two models, we present a comparison between the two with spatial and temporal steps $h = 1/8$, $\tau = 1/64$, $K_\alpha = K_\beta = 1.0$, and $\alpha = 1.0$ and $\beta = 1.8$ for different t on the domain $[-1, 1] \times [-1, 1]$ (Figure 5) and domain $[-2, 2] \times [-2, 2]$ (Figure 6). We see that as the domain size becomes larger the solution for the two models closer in agreement.
In order to see the effect of time on the difference between the two models, we present a comparison between the two with spatial and temporal steps $h = 1/8$, $\tau = 1/64$, $K_\alpha = K_\beta = 1.0$, and $\alpha = 1.0$ and $\beta = 1.8$ for different t on the domain $[-2, 2] \times [-2, 2]$ (Figure 7) and domain $[-3, 3] \times [-3, 3]$ (Figure 8). We see that as the time becomes larger the differences in the solution profiles for the two models becomes larger, however, extending the domain can reduce the difference between two models.
Figure 9 shows the error of solutions between the two models with spatial and temporal steps $h = 1/8$, $\tau = 1/64$, $K_\alpha = K_\beta = 1.0$, and $\alpha = 1.0$ and $\beta = 1.8$ for different t on the domain $[-2, 2] \times [-2, 2]$ and domain $[-3, 3] \times [-3, 3]$. We see that as the domain becomes larger the error becomes smaller.
We repeat these simulations, except now we replace the zero Dirichlet boundary condition by the homogeneous Neumann boundary condition

$$\frac{\partial M(\mathbf{r}, t)}{\partial \mathbf{r}}|_{\bar{\Omega}} = 0. \tag{48}$$

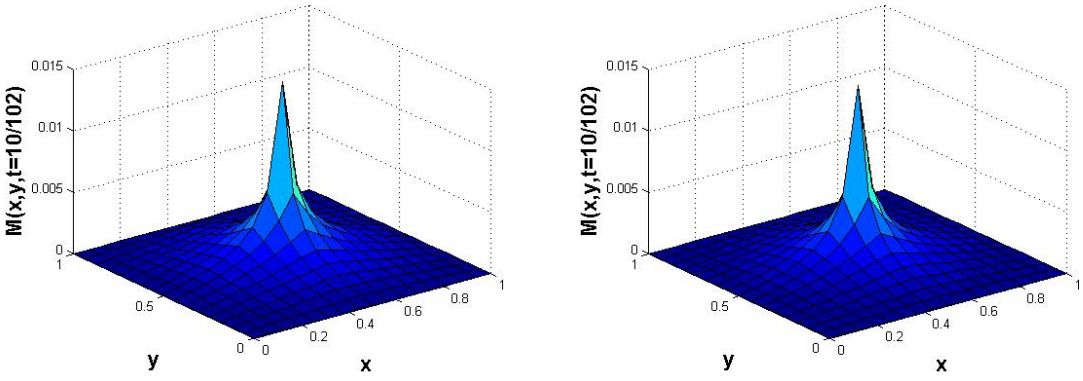

(a) (b)

Figure 4. The comparison of solution profiles between Models-1 and 2 with a nonlinear source term with spatial and temporal steps $h = 1/16$, $\tau = 1/102$ at time $t = 10/102$ with $K_\alpha = K_\beta = 1.0$, $t_{final} = 1.0$ for $\alpha = 0.5$ and $\beta = 1.5$. (a) Implicit numerical method. (b) Matrix transfer technique.

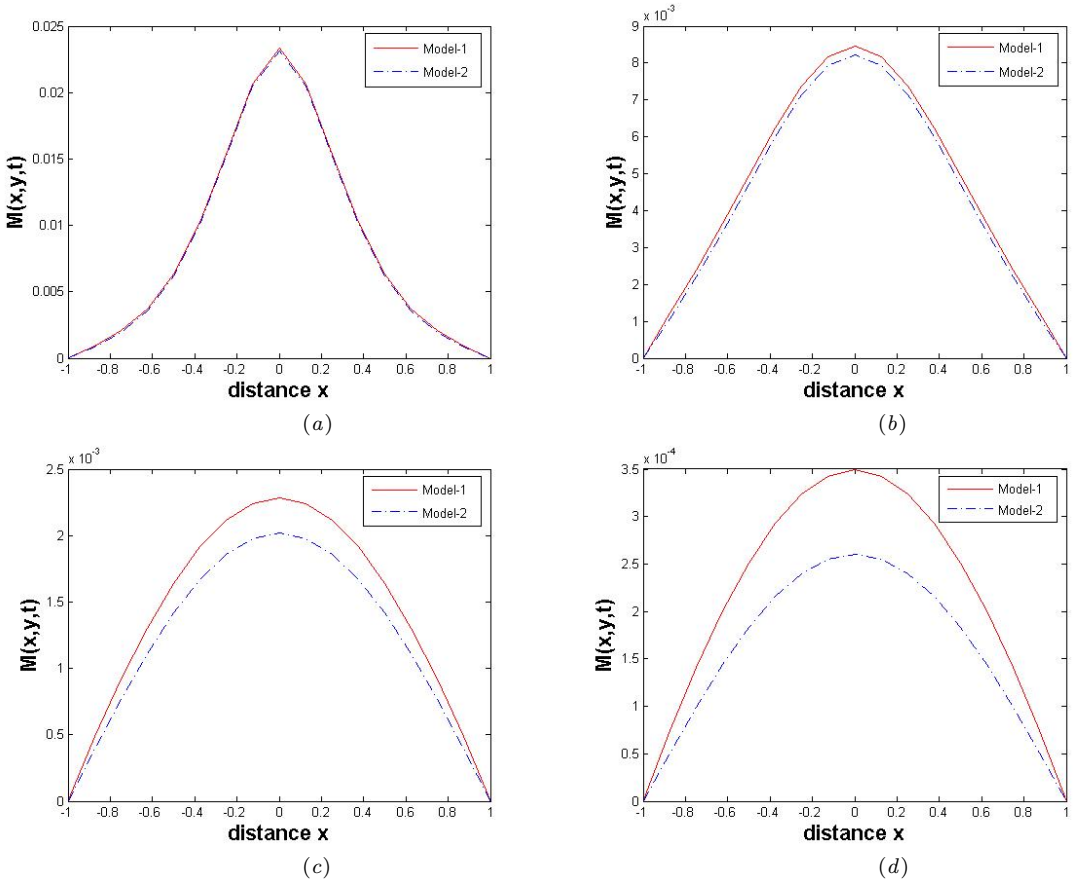

(a) (b)

(c) (d)

Figure 5. The comparison of solution profiles between Models-1 and 2 with a nonlinear source term with zero Dirichlet boundary condition with spatial and temporal steps $h = 1/8$, $\tau = 1/64$ at a finite rectangular region $[-1, 1] \times [-1, 1]$ with $K_\alpha = K_\beta = 1.0$ for $y = 0$, $\alpha = 1.0$ and $\beta = 1.8$ for different t.(a) $t = 0.1$. (b) $t = 0.2$. (c) $t = 0.5$. (d) $t = 1.0$.

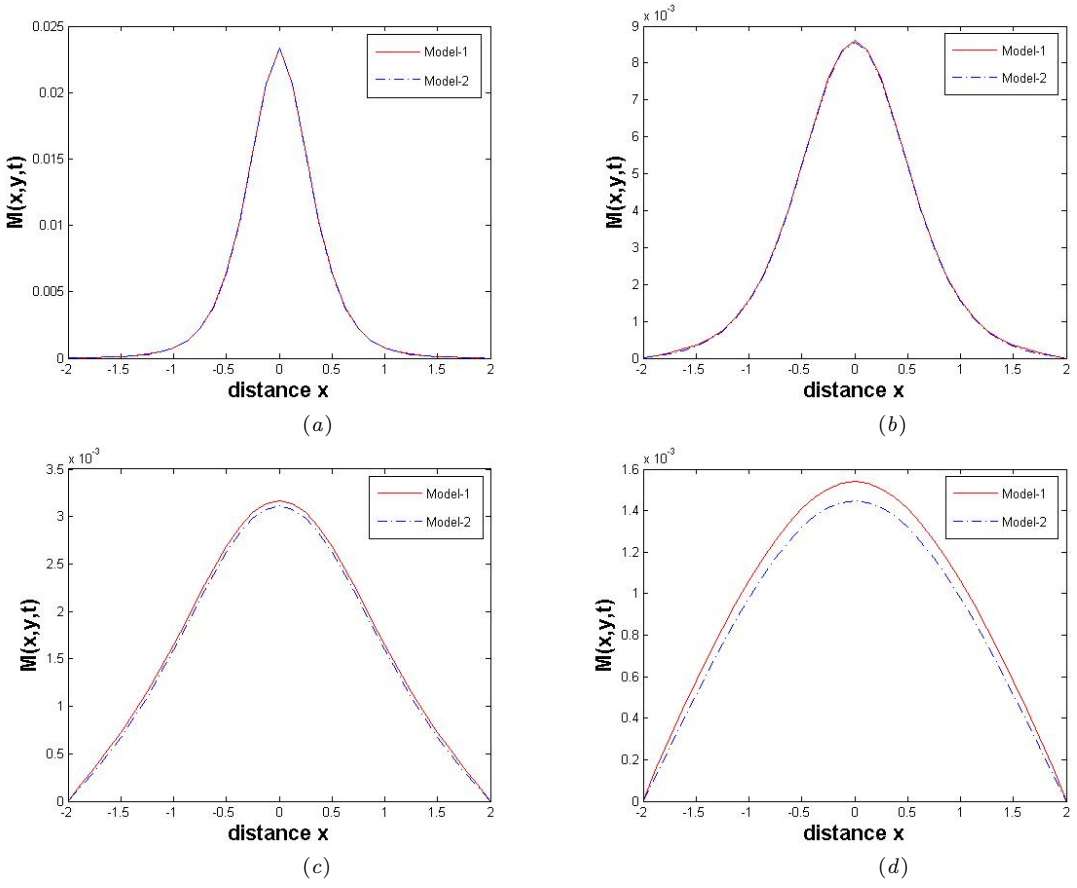

Figure 6. The comparison of solution profiles between Models-1 and 2 with a nonlinear source term with zero Dirichlet boundary condition with spatial and temporal steps $h = 1/8$, $\tau = 1/64$ at a finite rectangular region $[-2, 2] \times [-2, 2]$ with $K_\alpha = K_\beta = 1.0$ for $y = 0$, $\alpha = 1.0$ and $\beta = 1.8$ for different t.(a) $t = 0.1$. (b) $t = 0.2$. (c) $t = 0.5$. (d) $t = 1.0$.

Figures 10 and 11 give the dynamics for the domains $[-1, 1] \times [-1, 1]$ and $[-2, 2] \times [-2, 2]$, respectively. In this case, it can clearly be observed that the behaviour of the models, particularly at the boundaries at late times, is very different.

Finally, in Example 6.3 we give a comparison of the numerical solutions between Models-1 and 3 with a nonlinear source term.

Example 6.3.

$$Model-1: \quad \frac{\partial M(\mathbf{r},t)}{\partial t} = K_\beta\left(\frac{\partial^\beta}{\partial|x|^\beta} + \frac{\partial^\beta}{\partial|y|^\beta}\right)M(\mathbf{r},t) + f(M,\mathbf{r},t), \tag{49}$$

$$Model-3: \quad \frac{\partial M(\mathbf{r},t)}{\partial t} = -K_\beta(-\Delta)^{\frac{\beta}{2}}M(\mathbf{r},t) + f(M,\mathbf{r},t), \tag{50}$$

with initial and zero Dirichlet boundary conditions

$$M(\mathbf{r},0) = \delta(x-0.5, y-0.5), \tag{51}$$

$$M(\mathbf{r},t)|_{\bar{\Omega}} = 0, \tag{52}$$

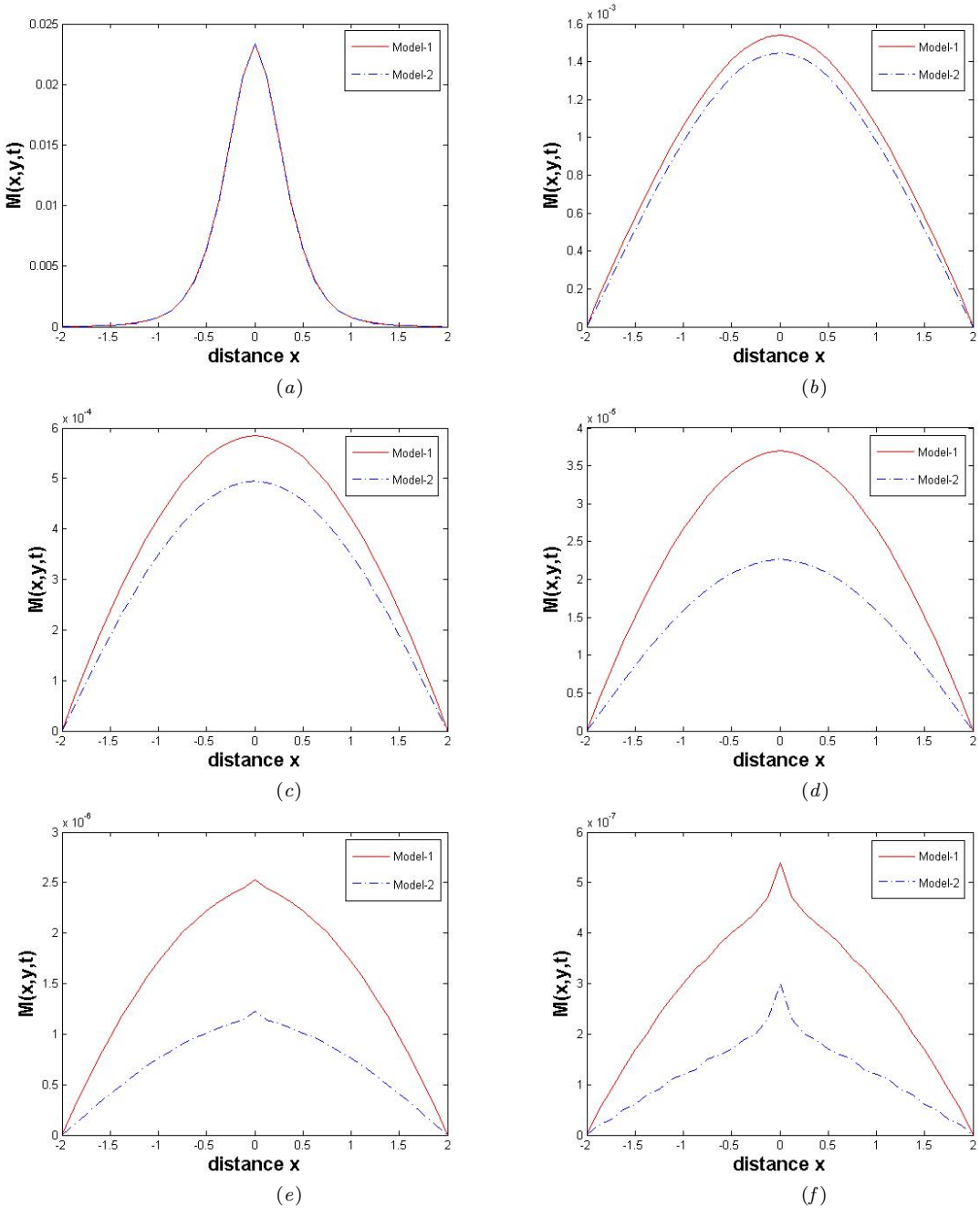

Figure 7. The comparison of solution profiles between Models-1 and 2 with a nonlinear source term with zero Dirichlet boundary condition with spatial and temporal steps $h = 1/8$, $\tau = 1/64$ at a finite rectangular region $[-2, 2] \times [-2, 2]$ with $K_\alpha = K_\beta = 1.0$ for $y = 0$, $\alpha = 1.0$ and $\beta = 1.8$ for different t.(a) $t = 0.1$. (b) $t = 1$. (c) $t = 2$. (d) $t = 5$. (e) $t = 8$. (f) $t = 10$.

where the nonlinear source term $f(M, \mathbf{r}, t)$ is Fisher's growth equation $f(M, \mathbf{r}, t) = 0.25M(\mathbf{r}, t)[1 - M(\mathbf{r}, t)]$, and $1 < \beta \leq 2$, $0 < t \leq T$, $\mathbf{r} = (x, y) \in \Omega$, Ω is the finite rectangular region $[0, 1] \times [0, 1]$ and $\bar{\Omega}$ is $\mathcal{R}^2 - \Omega$.
The comparison of solution profiles of equations (49) and (50) obtained by the implicit numerical method and matrix transfer technique, respectively, with spatial and temporal steps $h = 1/10$, $\tau = 1/100$ at time $t = 0.1$ with $K_\beta = 1.0$, $t_{final} = 1.0$ for $\beta = 1.8$ is given in Figure 12. From Figure 12, it can be seen clearly that the numerical

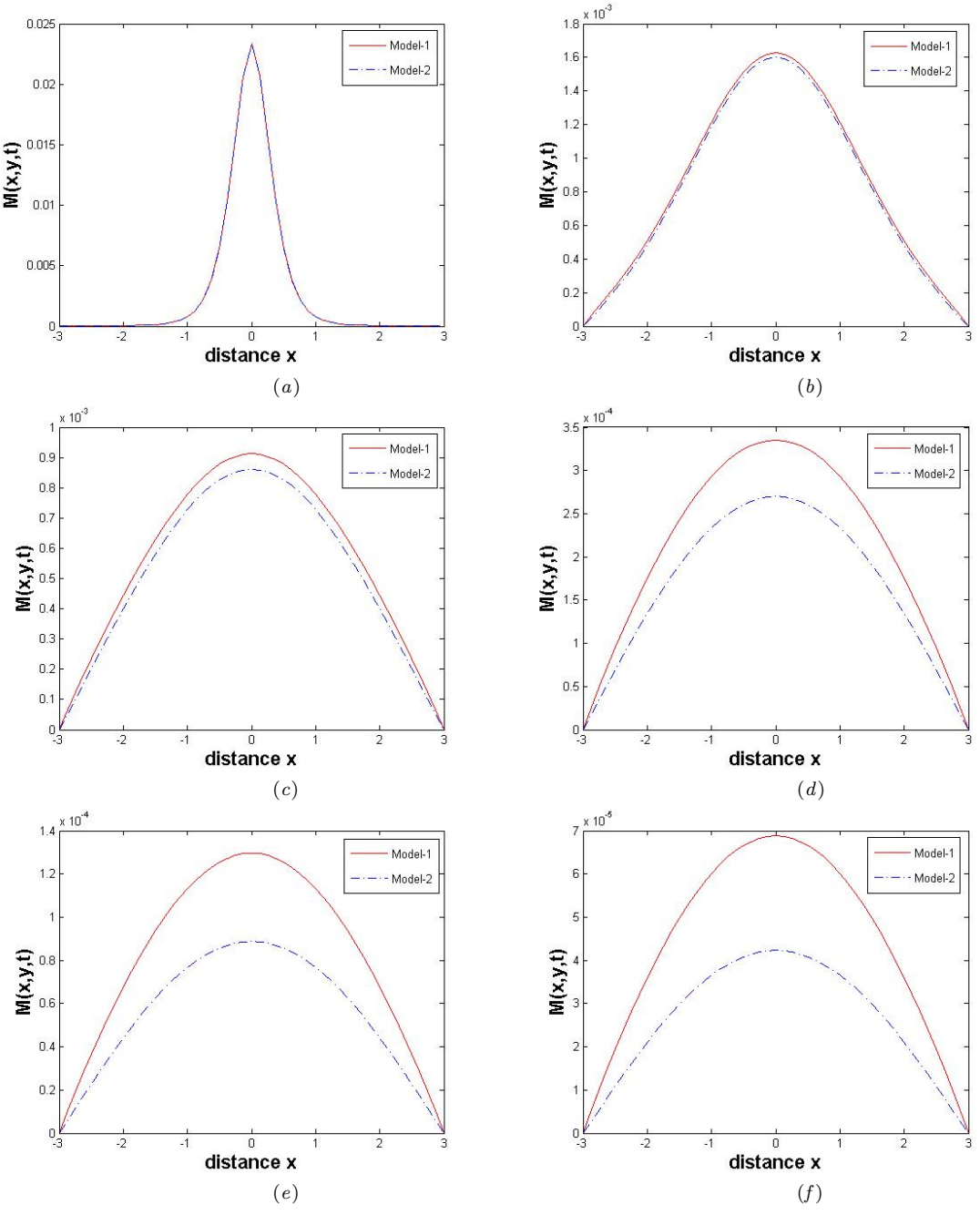

Figure 8. The comparison of solution profiles between Models-1 and 2 with a nonlinear source term with zero Dirichlet boundary condition with spatial and temporal steps $h = 1/8$, $\tau = 1/64$ at a finite rectangular region $[-3, 3] \times [-3, 3]$ with $K_\alpha = K_\beta = 1.0$ for $y = 0$, $\alpha = 1.0$ and $\beta = 1.8$ for different t.(a) $t = 0.1$. (b) $t = 1$. (c) $t = 2$. (d) $t = 5$. (e) $t = 8$. (f) $t = 10$.

solutions obtained from Model-3 are not in good agreement with those of the implicit numerical method from Model-1.

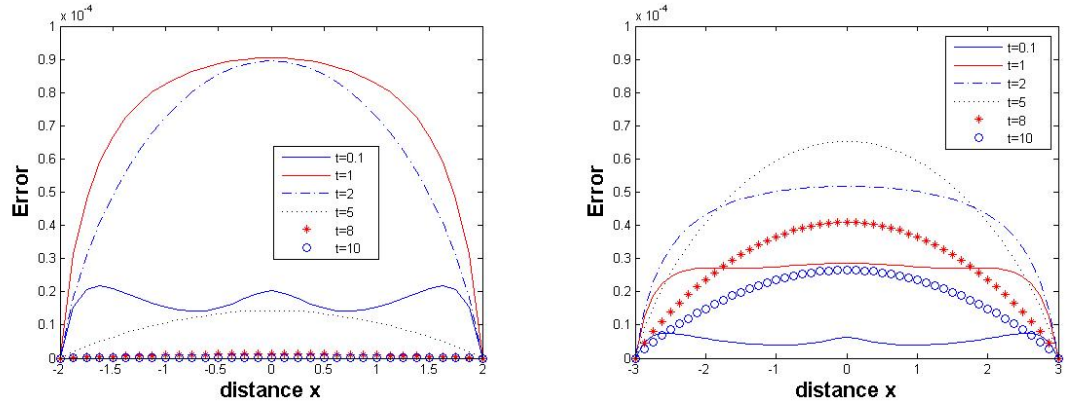

Figure 9. The error of solutions between Models-1 and 2 with a nonlinear source term with zero Dirichlet boundary condition with spatial and temporal steps $h = 1/8$, $\tau = 1/64$ with $K_\alpha = K_\beta = 1.0$ for $y = 0$, $\alpha = 1.0$ and $\beta = 1.8$ for different finite rectangular domains.(a) Finite rectangular region $[-2, 2] \times [-2, 2]$. (b) Finite rectangular region $[-3, 3] \times [-3, 3]$.

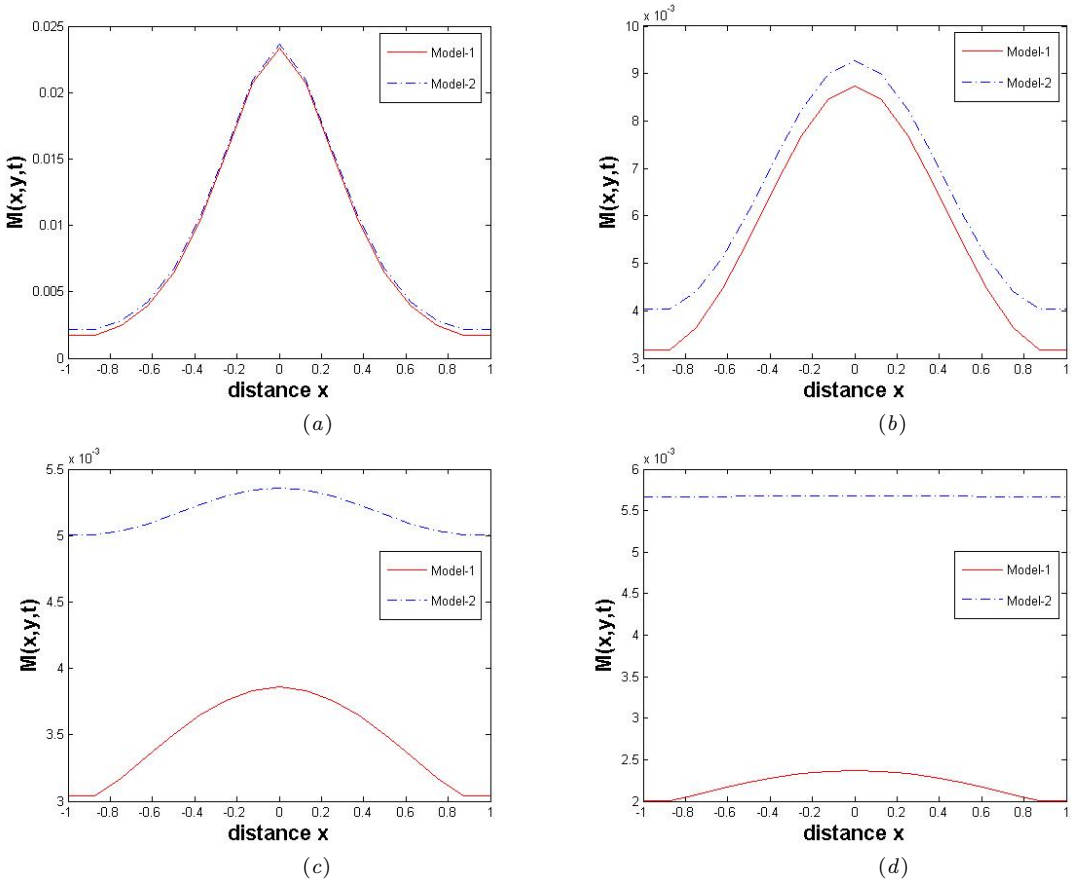

Figure 10. The comparison of solution profiles between Models-1 and 2 with a nonlinear source term with homogeneous Neumann boundary condition with spatial and temporal steps $h = 1/8$, $\tau = 1/64$ at a finite rectangular region $[-1, 1] \times [-1, 1]$ with $K_\alpha = K_\beta = 1.0$ for $y = 0$, $\alpha = 1.0$ and $\beta = 1.8$ for different t.(a) $t = 0.1$. (b) $t = 0.2$. (c) $t = 0.5$. (d) $t = 1.0$.

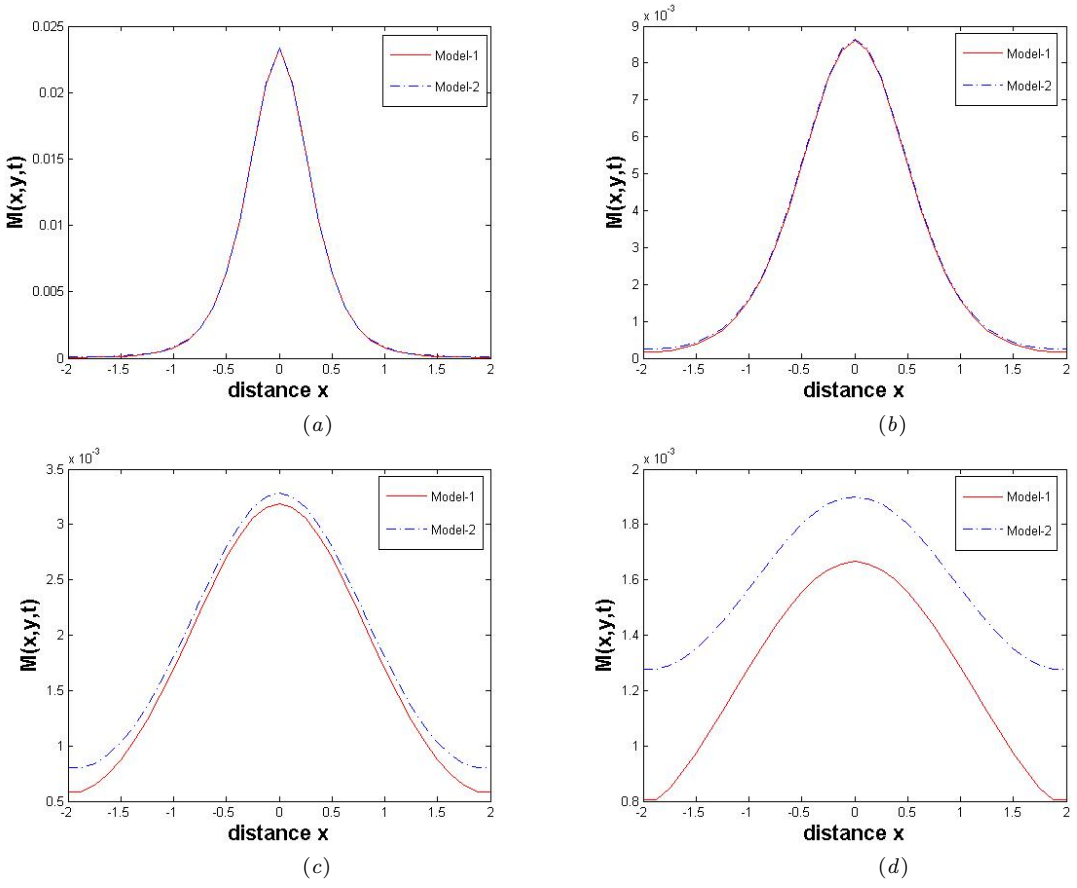

Figure 11. The comparison of solution profiles between Models-1 and 2 with a nonlinear source term with homogeneous Neumann boundary condition with spatial and temporal steps $h = 1/8$, $\tau = 1/64$ at a finite rectangular region $[-2, 2] \times [-2, 2]$ with $K_\alpha = K_\beta = 1.0$ for $y = 0$, $\alpha = 1.0$ and $\beta = 1.8$ for different t.(a) $t = 0.1$. (b) $t = 0.2$. (c) $t = 0.5$. (d) $t = 1.0$.

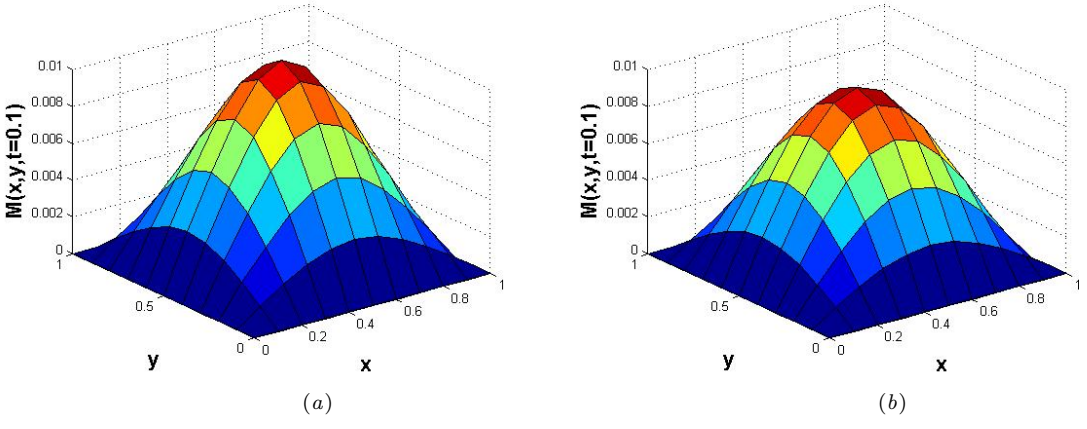

Figure 12. The comparison of solution profiles between Models-1 and 3 with a nonlinear source term with spatial and temporal steps $h = 1/10$, $\tau = 1/100$ at time $t = 0.1$ with $K_\beta = 1.0$, $t_{final} = 1.0$ for $\beta = 1.8$. (a) Implicit numerical method. (b) Matrix transfer technique.

7. Conclusions

In this paper, we compare the numerical solutions obtained from an implicit numerical method and the matrix transfer technique, for three types of space and time fractional Bloch-Torrey equations in two dimensions based on a Riesz derivative and two forms of a fractional Laplacian in one dimension and two dimensions, respectively. The main focus is on finite domains with zero Dirichlet boundary conditions. We show that these formulations are not equivalent, but that as the size of the domain increases, Model 1 and Model 2 are increasingly similar. However, this is not the case for homogeneous Neumann boundary conditions where Model 1 and Model 2 are very different. Furthermore, the one-dimensional and two-dimensional forms for the Laplacian can also be different even in the case of zero Dirichlet boundary conditions. This shows that the dynamics of fractional models very much depend on the boundary conditions in the case of finite domains, and that even in the case of zero Dirichlet boundary conditions we must take considerable care in deciding which model we should use and in interpreting the simulation results. In the future we plan to compare our methods for solving the space and time fractional models studied here with the methods proposed by Podlubny et al. [9]. However in that paper all examples are in one spatial dimension, although it is claimed that the approach is easily extendable to higher dimensions.

Acknowledgements

The authors gratefully acknowledge the help and interest in our work by Professor Kerrie Mengersen from QUT. Mr Yu also acknowledges the Centre for Complex Dynamic Systems Control at QUT for offering financial support for his PhD scholarship. This research was partially supported by the Australian Research Council grant DP120103770. We also thank the referees for their constructive comments and suggestions.

References

[1] I. Podlubny, Fractional Differential Equations, (Academic Press, New York, 1999)

[2] A. A. Kilbas, H. M. Srivastava and J. J. Trujillo, Theory and applications of fractional differential equations, (Elsevier, Amsterdam, 2006)

[3] R. Hilfer, Applications of fractional calculus in physics , (World Scientific Publishing, New York, 2000)

[4] R. Metzler and J. Klafter, Phys. Rep. 339, 1 (2000)

[5] G. Zaslavsky, Physics Reports 371(6), 461 (2002)

[6] R. Gorenflo, F. Mainardi, D. Moretti, and P. Paradisi, Nonlinear Dynamics 29, 129 (2002)

[7] M. M. Meerschaert and C. Tadjeran, Journal of Computational and Applied Mathematics 172, 65 (2004)

[8] Q. Yu, F. Liu, V. Anh, I. Turner, Internat. J. Numer. Meth. Eng. 74, 138 (2008)

[9] I. Podlubny, A. Chechkin, T. Skovranek, Y. Q. Chen, B. M. V. Jara, Journal of Computational Physics 228,

3137 (2009)

[10] K. Diethelm, The Analysis of Fractional Differential Equations: An Application Oriented Exposition Using Differential Operators of Caputo Type, (Springer, Berlin, 2010)

[11] A. Abragam, Principles of nuclear magnetism, (Oxford University Press, New York, 2002)

[12] H. C. Torrey, Physical Review 104(3), 563 (1956)

[13] S. Bhalekar, V. Daftardar-Gejji, D. Baleanu, and R. Magin, Computers and Mathematics with Applications 64(10), 3367 (2012)

[14] R. Magin, X. Feng, D. Baleanu, Concepts in Magnetic Resonance Part A 34A(1), 16 (2009)

[15] R. Magin, X. Feng, D. Baleanu, Magn. Reson. Engr. 34, 16 (2009)

[16] I. Petr*áš*, Computers and Mathematics with Applications 61(2), 341 (2011)

[17] R. Magin, W. Li, M. Velasco, J. Trujillo, D. Reiter, A. Morgenstern, and R. Spencer, Journal of Magnetic Resonance 210(2), 184 (2011)

[18] S. Bhalekar, V. Daftardar-Gejji, D. Baleanu, and R. Magin, Computers and Mathematics with Applications 61(5), 1355 (2011)

[19] V. M. Kenkre, E. Fukushima, and D. Sheltraw, Journal of Magnetic Resonance 128(1), 62 (1997)

[20] A. V. Barzykin, Phys. Rev. B 58(21), 14171 (1998)

[21] T. H. Jochimsena, A. Schäferb, R. Bammera, and M. E. Moseleya, Journal of Magnetic Resonance 180(1), 29 (2006)

[22] Q. Yu, F. Liu, I. Turner and K. Burrage, Applied Mathematics and Computation 219, 4082 (2012)

[23] Q. Yu, F. Liu, I. Turner and K. Burrage, Phil Trans R Soc A 20120150 (2013)

[24] R. Magin, O. Abdullah, D. Baleanu, and X. Zhou, Journal of Magnetic Resonance 190(2), 255 (2008)

[25] X. Zhou, Q. gao, O. Abdullah, and R. Magin, Magnetic Resonance in Medicine 63(3), 562 (2010)

[26] M. Ilic, F. Liu, I. Turner, and V. Anh, Fractional Calculus and Applied Analysis 9(4), 333 (2006)

[27] Q. Yang, I. Turner, F. Liu, and M. Ilic, SIAM J. Sci. Comput., 33(3), 1159 (2011)

[28] K. Burrage, N. Hale, and D. Kay, SIAM J. SIAM J. Sci. Comput., 34(4), A2145 (2012)

[29] A. Bueno-Orovio, D. Kay, and K. Burrage, Journal of Computational Physics (2012) (in press)

[30] P. Zhuang, F. Liu, V. Anh, and I. Turner, SIAM J. Numer. Anal. 47(3), 1760 (2009)

[31] Q. Yang, F. Liu, and I. Turner, Applied Mathematical Modelling 34(1), 200 (2010)

[32] S. Shen, F. Liu, and V. Anh, Numerical Algorithms 56(3), 383 (2011)

[33] M. D. Ortigueira, International Journal of Mathematics and Mathematical Sciences 2006, 48391 (2006)

[34] C. Celik, and M. Duman, Journal of Computational Physics 231, 1743 (2012)

[35] F. Liu, and K. Burrage, Computer & Mathematics with Application 62, 822 (2011)

[36] F. Liu, P. Zhuang, V. Anh, I. Turner, and K. Burrage, Applied Mathematics and Computation 191, 12 (2007)